The Journal of Experimental Biology 209, 2452-2461
Published by The Company of Biologists 2006
doi:10.1242/jeb.02275

Silken toolkits: biomechanics of silk fibers spun by the orb web spider *Argiope argentata* (Fabricius 1775)

Todd A. Blackledge[1,*] and Cheryl Y. Hayashi[2]

[1]*Department of Biology, University of Akron, Akron, OH 44325-3908, USA and* [2]*Department of Biology, University of California, Riverside, CA 92521, USA*

*Author for correspondence (e-mail: blackledge@uakron.edu)

Accepted 18 April 2006

Summary

Orb-weaving spiders spin five fibrous silks from differentiated glands that contain unique sets of proteins. Despite diverse ecological functions, the mechanical properties of most of these silks are not well characterized. Here, we quantify the mechanical performance of this toolkit of silks for the silver garden spider *Argiope argentata*. Four silks exhibit viscoelastic behaviour typical of polymers, but differ statistically from each other by up to 250% in performance, giving each silk a distinctive suite of material properties. Major ampullate silk is 50% stronger than other fibers, but also less extensible. Aciniform silk is almost twice as tough as other silks because of high strength and extensibility. Capture spiral silk, coated with aqueous glue, is an order of magnitude stretchier than other silks. Dynamic mechanical properties are qualitatively similar, but quantitatively vary by up to 300% among silks. Storage moduli are initially nearly constant and increase after fiber yield, whereas loss tangents reach maxima of 0.1–0.2 at the yield. The remarkable mechanical diversity of *Argiope argentata* silks probably results in part from the different molecular structures of fibers and can be related to the specific ecological role of each silk. Our study indicates substantial potential to customize the mechanics of bioengineered silks.

Key words: Araneidae, capture spiral, dynamic mechanical analysis, flagelliform silk, major ampullate silk, polymer, silver garden spider, *Argiope argentata*.

Introduction

Spider silk is an inspiration for biomimetic super fibers because of the high tensile strength and unmatched toughness of major ampullate draglines (Kaplan et al., 1994; Vollrath, 1999). Silk also provides ecologists with links between the behaviors of spiders as they spin webs and selective factors in the environment (Blackledge et al., 2003; Blackledge and Gillespie, 2004; Craig, 2003). Molecular biologists are increasing the known diversity of genes that code for a variety of spider silk proteins, whereas biochemists and structural biologists develop hypotheses for how amino acid sequence affects the mechanical function of silk fibers (e.g. Gatesy et al., 2001; Guerette et al., 1996; Hayashi and Lewis, 1998; Simmons et al., 1996; Tian and Lewis, 2005). Finally, the mechanical process of spinning fibers from liquid dope has been studied from both morphological and functional perspectives (Garrido et al., 2002; Vollrath and Knight, 1999; Vollrath et al., 1998; Vollrath et al., 2001) and genetic engineers are synthesizing recombinant silk proteins (Arcidiacono et al., 1998; Foo and Kaplan, 2002; Huemmerich et al., 2004; Lazaris et al., 2002; Lewis et al., 1996; Winkler et al., 1999). Together, these disparate fields of research indicate the potential of the spider silk system to integrate aspects of organismal biology, molecular evolution and biomechanics (e.g. Craig, 2003; Gosline et al., 1999; Hayashi et al., 1999).

Characterization of the mechanical performance of different types of spider silk fibers is a crucial first step for developing hypotheses that relate protein sequence and structure to the ecological function of spider silk. For instance, several studies have demonstrated that orb webs contain two types of silk fibers with radically different mechanical properties. The framework of webs is composed of stiff and strong major ampullate silk. By contrast, the sticky capture spiral is an order of magnitude stretchier and 1000 times more compliant than major ampullate silk (Denny, 1976; Gosline et al., 1999; Kitagawa and Kitayama, 1997; Köhler and Vollrath, 1995). These silks function together to arrest and absorb the kinetic energy of flying insects. However, most spiders spin more than one or two types of silk. Orb-weaving spiders spin a total of seven different kinds of silk, five of which form long fibers (Foelix, 1996). Whereas capture, spiral and major ampullate silks are moderately well characterized, comparative data on the mechanical performance of other silks are limited (Denny,

1976; Stauffer et al., 1994). However, several lines of evidence predict that these silks are also likely to have evolved diverse mechanical properties. Each type of fiber is used for specific tasks by spiders and is extruded from the spinnerets of spiders through discrete spigots that are attached to individual silk glands. Each type of silk gland differs from the others in size, location and morphology. Finally, amino acid composition analyses and studies of silk transcripts from these glands suggest that each type of silk is composed of a unique set of proteins (Garb and Hayashi, 2005; Gatesy et al., 2001; Hayashi et al., 2004).

Here, we present a detailed mechanical characterization of all five fibrous silks spun by an orb-weaving spider, *Argiope argentata* (Fabricius 1775) to test the hypothesis that each of these biochemically distinct silks has unique mechanical properties. We then use these data to suggest relationships between the molecular architecture, mechanical performance, and ecological function of these fibers. These hypotheses lay the foundation for studies to better understand why spiders have evolved such diverse toolkits of silk.

Materials and methods

Collection of silk

Eighteen adult *Argiope argentata* (Fabricius 1775) were collected in the field (Encinitas, CA, USA) as mature or penultimate females and housed individually in the laboratory in 60 cm×60 cm×13 cm cages. Silks were obtained from spiders within 3 weeks after capture, during which time spiders were fed a combination of house crickets *Acheta domesticus* (L. 1758) and honey bees *Apis mellifera* L. 1758. Ambient temperature in the laboratory ranged from 21–22°C and humidity varied from 20–70%.

We collected major and minor ampullate silk from restrained spiders using forcible silking as previously described (Blackledge et al., 2005c). Capture spiral silk was harvested directly from the outermost spirals of freshly spun webs. Individual aciniform silk fibers were collected by first throwing crickets into webs to induce prey wrapping attacks by spiders. We then inserted '**y**' shaped pieces of cardboard between the spiders and prey such that the spiders continued to wrap silk around the cardboard. After the spider had wrapped the cardboard with one or two layers of silk, we isolated individual fibers for testing by first gently pulling away adjacent fibers, taking care not to touch or pull upon the fiber of interest, until a single discrete fiber spanning the '**y**' remained. We then adhered this single fiber to the same type of cardboard mount previously used to test other silk (Hayashi et al., 2004). Tubuliform fibers were collected from the inner flocculent silk of egg sacs, from a region similar to that described as the second insulation layer for *Zygiella x-notata* (Clerk 1757) egg sacs (Gheysens et al., 2005). We first cut open the tough outer layer of the egg sacs and removed the eggs. We then gently pulled the bulk of the flocculent silk free from the outer covering and separated a few fibers from the larger mass under a dissecting microscope. This allowed us to gently pull free up to several cm of a single fiber, without tensing it (as inferred because the fiber retained its crimped or curled shape throughout the entire process until secured to the mount). Finally, we secured that single fiber to the same type of cardboard mounts as previously described. Care was taken to ensure that fibers were not stressed during collection and that only single fibers with no attachments to other fibers were used.

Silks were secured to cardboard mounts using cyanoacrylate glue (SuperGlue^{TM}), except for capture spiral silk, the only wet silk, which was affixed using water-based Elmer's^{TM} glue. Gage lengths were 21 mm for major ampullate, most capture spiral, tubuliform, and minor ampullate silk. Aciniform and some capture spiral silks were mounted using 10 mm gage lengths.

Mechanical analysis of silk

Silks were tested in the laboratory on the same day they were collected. We used polarized light microscopy to measure the diameters of all threads prior to testing because this technique allowed us to control for variation between samples in cross-sectional area (Blackledge et al., 2005a). Morphological studies demonstrate that spider silk fibers can exhibit mild to moderate shape anisotropy, such that they are elliptical rather than circular in cross-section (Pérez-Rigueiro et al., 2001), and that the diameters of threads can also vary along their length (Madsen and Vollrath, 2000). However, we measured the diameter of each fiber at nine different locations to control for this variability, thereby allowing us to estimate the average cross-sectional area of each fiber using a single value (Blackledge et al., 2005a; Dunaway et al., 1995). The diameters of the four types of dry silk were measured directly. For capture spiral silk, we collected pairs of contiguous samples of capture spiral from webs. The first sample of each pair was mechanically characterized and its diameter estimated by laying the second sample onto a glass slide and measuring the diameters of the second sample's core fibers (Blackledge et al., 2005a).

Quasistatic load-extension data and dynamic data were generated using a Nano Bionix tensile tester (MTS Systems Corp., Oak Ridge, TN, USA), with a load resolution of 50 nN and an extension resolution of 35 nm. Fibers were extended at a constant rate of 1% strain per second, until failure (Blackledge et al., 2005b; Blackledge et al., 2005c). We then transformed raw load-extension data into true stress (σ_t), as:

$$\sigma_t = F / A ,$$

where F is the force applied to the specimen and A is the estimated cross-sectional area of the specimen calculated from the original cross-sectional area under an assumption of constant volume (Vollrath et al., 2001), and true strain (ϵ_t), as:

$$\epsilon_t = \log_e (L / L_o) ,$$

where L is the instantaneous length of the fiber at each extension value and L_o is the original gage length of the fiber. Using true stress and true strain provides a less biased comparison among fibers that differ in extensibilities compared

to using engineering stress and engineering strain (Blackledge et al., 2005c; Köhler and Vollrath, 1995; Opell and Bond, 2001). We therefore chose to concentrate our data analysis on the true stress and true strain characteristics of fibers. However, we also provide the engineering stress and engineering strain data to facilitate easy comparison to past research on fiber biomechanics. We used true stress and true strain to compute the initial stiffness of fibers (Young's modulus), how far fibers stretched before breaking (extensibility) and the ultimate strength of fibers. We also calculated the energy that fibers absorbed before breaking (toughness), which is unaffected by the use of true *versus* engineering values.

We calculated several measures of how fibers absorb energy using continuous dynamic analysis (CDA). The Nano Bionix performs CDA by imposing a tiny dynamic oscillation upon fibers during extension. This provides a continuous measure of the amount of energy stored within silk fibroins (E' or storage modulus) as a result of deformation of chemical bonds (Sirichaisit et al., 2000; Termonia, 1994) and entropic effects (Gosline et al., 1984), as well as the ratio of the viscous to elastic behavior of the fibers (tan δ or loss tangent). We used a dynamic strain oscillation frequency of 20 Hz and dynamic force amplitude of 4.5 mN, resulting in a maximum dynamic displacement of 45 μm. We chose to compare these values among silks at three different points – the initial values while fibers were still in the elastic region, the maximum value of the loss tangent, which corresponds to the yield point (Blackledge et al., 2005c), and the final values just prior to failure of the fibers. More details on these methods and how to interpret data from CDA are presented in an earlier study (Blackledge et al., 2005c).

Statistical analysis

For each type of silk, we tested the performance of many samples of silk from each individual spider. Therefore, all analyses were performed using the mean performance characteristics for individual spiders to prevent pseudoreplication. We first used a MANOVA to test the hypothesis that the five types of silk differed in their quasistatic material properties. We then used one-way ANOVAs to compare individual quasistatic properties among the five types of silk. Dynamic data were much more difficult to obtain than the traditional quasistatic data, which resulted in substantially smaller sample sizes. Therefore, data from all fibers were pooled, rather than using the means of individual spiders, for our calculations of mean and s.e.m. such that these data are presented for descriptive purposes and are not compared statistically.

Results

All five types of fibrous silk spun by *Argiope argentata* exhibited quantitative differences in mechanical properties (Table 1 and Figs 1, 2). The stress-strain behavior of major ampullate, tubuliform, minor ampullate and aciniform silk, were typical of many viscoelastic polymers (Figs 1 and 2).

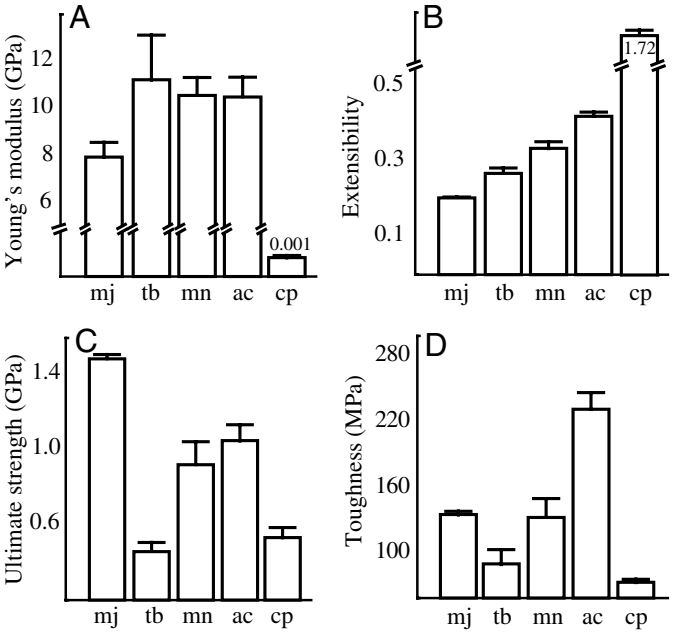

Fig. 1. Quasistatic mechanical properties of each type of fibrous silk spun by *Argiope argentata* (mean ± s.e.m.). Standard errors were calculated using individual spiders, rather than total numbers of fibers tested, as the sampling unit. See Table 1 for sample sizes. ac, aciniform; cp, capture spiral; mj, major ampullate; mn, minor ampullate; tb, tubuliform.

Stress initially increased linearly for the first 1–2% strain until fiber yield began. The yield sometimes consisted of little more than a slight decrease in the slope of the stress-strain curve for major ampullate silk, whereas by contrast, stress often decreased during yield for aciniform and minor ampullate silk. Tubuliform fibers always displayed a distinct yield region characterized by a strong decrease in the slope of the stress-strain curve, although never below a slope of zero. After yield, these four silks continued to extend at relatively constant stiffness, except for minor ampullate fibers, which exhibited increased hardening near failure (Fig. 2).

The diameters of single fibers varied significantly among types of silk (Fig. 3; ANOVA, $F_{4,21}$=34, P<0.00001). Major ampullate and capture spiral fibers were similar in diameter (3.5±0.2 μm and 3.5±0.4 μm). Tubuliform fibers were thicker than other types of silk (5.3±0.8 μm). Aciniform fibers were exceptionally fine (0.33±0.02 μm) whereas minor ampullate fibers were slightly thicker (1.1±0.7 μm) but not significantly different from aciniform fibers due to their variability.

Our data reveal an impressive range of mechanical and material properties that differed significantly among the diverse silks spun by *Argiope* (MANOVA, $F_{4,16}$=714, P<0.00001). Individual silks varied in stiffness, extensibility, strength, and toughness (univariate ANOVAs, F values ranged from 175 to 441, d.f.=4, 27, all P<0.01). Tubuliform fibers had the highest stiffness of all the silks before the yield region, but they also exhibited the lowest stiffness after the yield region. Capture spiral was 1000 times more compliant than all other

Table 1. *Quasistatic material properties of silk spun by Argiope argentata compared to other araneid spiders*

Silk	Young's modulus (GPa)	True values: Ultimate strength (MPa)	True values: Extensibility (mm/mm)	Engineering values: Ultimate strength (MPa)	Engineering values: Extensibility (mm/mm)	Toughness (J cm^{-3})	Source
Major ampullate (*N*=5, *n*=135)	8.0±0.8	1495±65	0.205±0.005	1217±56	0.228±0.007	136±7	This study
Araneus sericatus (*n*=15)	8.6±–	880±–	0.22±–	710±–	0.24±–	106±–	(Denny, 1976)
Araneus diadematus (*n*=6)	1.2±0.2	1154±14	0.33±0.02	824±10	0.40±0.03	194±–	(Köhler and Vollrath, 1995)
Araneus gemmoides (*n*=10)	–	4700±500	0.23±0.05	–	–	–	(Stauffer et al., 1994)
Argiope trifasciata (*n*=28)	6.9±0.4	–	–	600±50	0.30±0.02	90±10	(Pérez-Rigueiro et al., 2001)
Tubuliform (*N*=4, *n*=29)	11.6±2.1	476±90	0.2857±0.015	360±70	0.337±0.019	95±17	This study
Araneus gemmoides (*n*=10)	–	2300±200	0.19±0.02	–	–	–	(Stauffer et al., 1994)
Araneus diadematus (*n*~400)	8.7±0.1	–	–	270±3	0.32±0.01	–	(Van Nimmen et al., 2005)
Minor ampullate (*N*=8, *n*=51)	10.6±1.2	923±154	0.330±0.033	669±113	0.401±0.047	137±22	This study
Argiope trifasciata (*n*=11)	8.9±0.5	–	–	483±34	0.556±0.04	150±12	(Hayashi et al., 2004)
Araneus gemmoides (*n*=10)	–	1400±100	0.22±0.07	–	–	–	(Stauffer et al., 1994)
Araneus diadematus (*n*=55)	–	–	–	–	0.34±–	–	(Work, 1977)
Aciniform (*N*=6, *n*=28)	10.4±1.4	1052±120	0.404±0.024	636±78	0.505±0.039	230±31	This study
Argiope trifasciata (*n*=10)	9.8±1.1	–-	–	687±56	0.83±0.06	376±39	(Hayashi et al., 2004)
Capture spiral (*N*=5, *n*=87)	0.001±0.0001	534±40	1.72±0.05	95±9	4.65±0.26	75±6	This study
Araneus sericatus (*n*=41)	–	1270±45	1.19±0.05	296±10	3.29±0.32	150±9	(Denny, 1976)
Araneus diadematus (*n*=6)	–	1338+80	1.75±0.15	233±14	4.75±0.16	283±18	(Köhler and Vollrath, 1995)

All values are means ± s.e.m. For data from this study, s.e.m. was calculated using individual spiders (*N*) as the sampling unit, while values from most of the other studies utilized the total number of fibers tested (*n*). –, data were not obtained.

silks (Tukey's Honest Significant Differences *post-hoc* comparison $P<0.01$). Capture spiral was also the most extensible silk (Tukey's Honest Significant Differences *post-hoc* comparison $P<0.0005$); stretching to a true stain of more than 1.0 before it gradually stiffened and finally broke at roughly 450% of its original length. Major ampullate silk was, by far, the strongest silk with an ultimate strength of 1.5 GPa (Tukey's Honest Significant Differences *post-hoc* comparison $P<0.05$). However, major ampullate silk was also less extensible than all other fibers except for tubuliform silk (Tukey's Honest Significant Differences *post-hoc* comparison $P<0.01$). Finally, aciniform silk was approximately 2–3 times as tough as other silks (Table 1 and Fig. 1; Tukey's Honest Significant Differences *post-hoc* comparison $P<0.01$).

There were striking similarities in the qualitative dynamic behavior of the four types of dry silk, but there were also substantial quantitative differences (Figs 4 and 5). Loss tangent (tan δ) was initially low and constant for the first 1% of strain and then increased to a maximum around fiber yield before decreasing gradually until failure. Storage modulus (E') was initially constant or decreased slightly through yield before increasing linearly until failure. Tubuliform silk was distinct from other fibers in its relatively small increase in storage modulus during extension and by its nearly constant loss tangent after yield. Tubuliform fibers also had a much lower loss tangent than other silks throughout the elastic and yield regions (Table 2, Fig. 5).

The dynamic behavior of capture spiral silk differed from that of the dry silks. Storage modulus was near zero until capture spiral fibers were extended at least 100% and began to stiffen. Storage modulus then gradually increased until failure, but still reached only half that of dry silks, with the exception of tubuliform fibers (Figs 4,5). By contrast to dry silks, the slope of storage modulus continued to increase until failure. Because of its extremely low loss modulus, we could only obtain data on the loss tangent of capture spiral near failure. However, the loss tangent of capture spiral at failure was similar to that of major ampullate silk.

Discussion

Each of the five fibrous silks spun by *Argiope argentata* had a distinct suite of mechanical properties (Figs 1–5). Comparing the four dry silks (aciniform, major ampullate minor

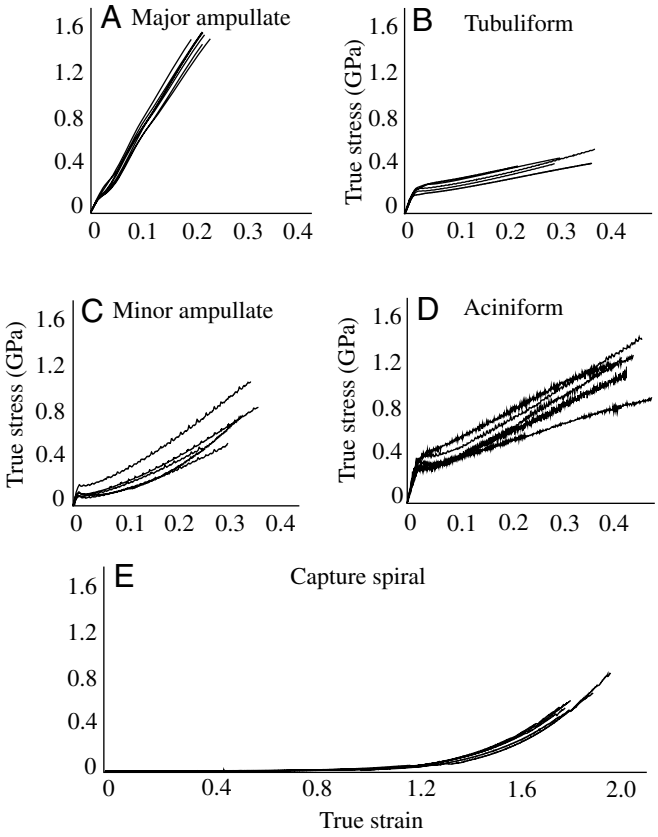

Fig. 2. Typical stress–strain curves for each of the five fibrous silks spun by *Argiope argentata*. Five tests are shown for each silk. Note the difference in the magnitude of the *x* axis for most types of silk (A–D) relative to capture spiral silk (E).

ampullate and tubuliform), major ampullate silk was the least stiff and least extensible whereas aciniform silk was the most extensible; major ampullate silk was the strongest, whereas tubuliform silk was the weakest; and finally, tubuliform silk had the lowest toughness whereas aciniform fibers had the highest toughness. The only wet silk, capture spiral, was three orders of magnitude more compliant and one order of magnitude stretchier than the dry silks. The dynamic properties of the four dry silks were qualitatively similar to one another (Fig. 5), and to major ampullate silk from the western black widow *Latrodectus hesperus* Chamberlin and Ivie 1935 (Blackledge et al., 2005c). By contrast to the dynamic behavior of the four dry silks, capture spiral silk had an extremely low storage modulus that rapidly increased as the fiber stiffened just prior to failure (Fig. 5).

In general, our mechanical data agree with the results of previous research on silks spun by other species of orb-weaving spiders (Table 1). Exceptions are the analyses of silks from *Araneus gemmoides* Chamberlin and Ivie 1935 and *Nephila clavipes* L. 1767 (Stauffer et al., 1994). Stauffer et al. found much greater tensile strength for major ampullate, minor ampullate and tubuliform silk than our values, as well as much lower extensibilities for minor ampullate and tubuliform silk.

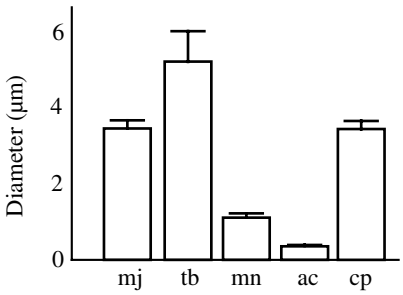

Fig. 3. Diameters of single fibers (mean ± s.e.m.) for each of the different types of silks spun by *Argiope argentata*. Standard errors were calculated using individual spiders, rather than total numbers of fibers tested, as the sampling unit. See Table 1 for sample sizes. ac, aciniform; cp, capture spiral; mj, major ampullate; mn, minor ampullate; tb, tubuliform.

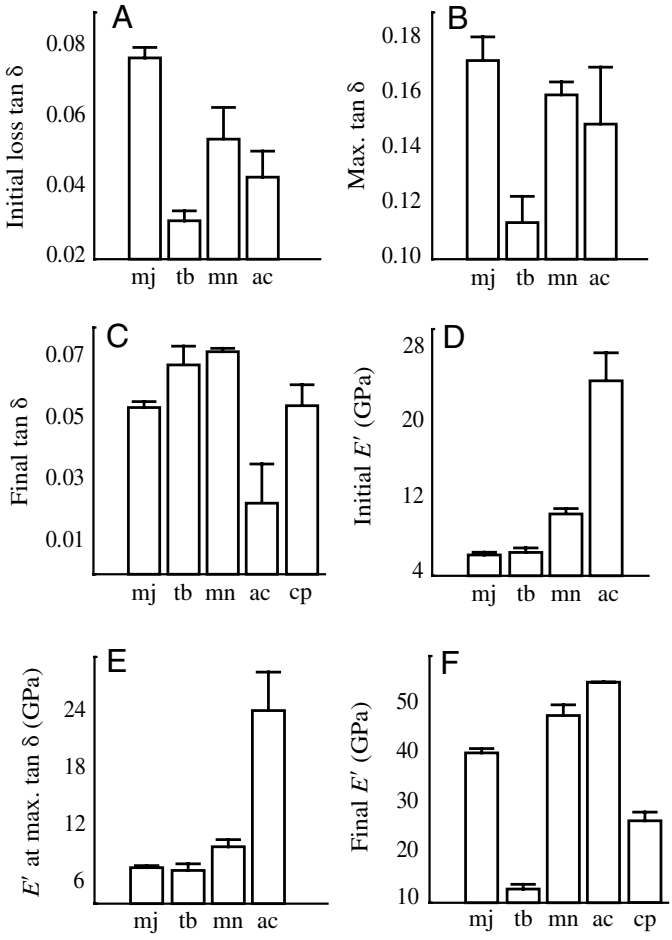

Fig. 4. Dynamic mechanical properties of each type of fibrous silk spun by *Argiope argentata* (mean ± s.e.m.). For these data only, s.e.m. was calculated using the total number of fibers tested as the sampling unit, rather than individual spiders. Properties for capture spiral were measurable only at high strain. See Table 2 for sample sizes. *E′*, storage modulus; tan δ, loss tangent; ac, aciniform; cp, capture spiral; mj, major ampullate; mn, minor ampullate; tb, tubuliform.

Table 2. *Dynamic material properties of silk spun by Argiope argentata and the western black widow Latrodectus hesperus*

Silk	Loss tangent			Storage modulus (GPa)			Source
	Initial	Max	Final	Initial	At max. loss tan	Final	
Major ampullate (*N*=4, *n*=27)	0.077±0.003	0.172±0.009	0.054±0.002	6.2±0.3	7.8±0.2	40.4±0.9	This study
Latrodectus hesperus (*n*=12)	0.063±0.007	0.197±0.009	0.075±0.003	8.7±1.1	10.6±0.8	47.6±3.3	(Blackledge et al., 2005c)
Tubuliform (*N*=1, *n*=6)	0.031±0.003	0.113±0.010	0.068±0.006	6.5±0.5	7.5±0.7	12.8±1.0	This study
Minor ampullate (*N*=2, *n*=6)	0.054±0.009	0.160±0.005	0.072±0.001	10.5±0.6	10.0±0.8	48.0±2.2	This study
Aciniform (*N*=1, *n*=2)	0.043±0.007	0.149±0.021	0.023±0.013	24.6±3.0	24.4±4.1	54.7±0.0	This study
Capture spiral (*N*=1, *n*=6)	–	–	0.057±0.011	–	–	24.5±1.8	This study

All values are mean ± s.e.m. For these data only, s.e.m. was calculated using the total number of fibers tested (*n*) as the sampling unit rather than individual spiders (*N*). –, data were not obtained.

All silks are from *Argiope argentata*, except major ampullate silk from *Latrodectus hesperus*.

Although these differences may represent real variation among species, disparities between our methodologies provide possible alternative explanations. Stauffer et al. extended fibers six times slower than we did, although slower strain rates typically increase, rather than decrease, extensibility (e.g. Cunniff et al., 1994). We used polarized light microscopy to compute diameters from nine measurements averaged for every fiber tested (Blackledge et al., 2005a). By contrast, Stauffer et al. estimated diameters of fiber bundles using density and mass or sometimes using microprojection of exemplar fibers and choosing the smallest measurement, which could increase calculation of tensile strength. However, even if we utilized our smallest diameter measurements for each fiber, our ultimate strength values would still not approach those of Stauffer et al. Instead, a combination of methodological differences may explain the dissimilarity of the Stauffer et al. results to the values that were found by a number of other researchers including us. For example, the 4–5 GPa ultimate strength that Stauffer et al. recorded for major ampullate silk is much higher than has been found in a range of studies by other researchers. By contrast, our value of 1.2 GPa is well within the 0.8–1.5 GPa range of engineering stress for ultimate strength that is typically reported for orbicularian major ampullate silk (Table 1) (Blackledge et al., 2005c; Gosline et al., 1994; Kitagawa and Kitayama, 1997; Madsen and Vollrath, 2000; Work, 1976).

Details of the silk collection method can affect the mechanical properties of silk fibers (Garrido et al., 2002; Madsen and Vollrath, 2000; Ortlepp and Gosline, 2004). However, even though we used several techniques to obtain the five types of silks in our study, differences in collection methods seem unlikely to account for most of the variation in mechanical performance. Consider that major and minor ampullate fibers were collected using identical forcible silking techniques but differed in every characteristic except toughness (Fig. 1). Additionally, aciniform and tubuliform fibers were both collected from natural sources (i.e. not forcibly silked) by teasing individual fibers out of large bundles or swaths of silk, yet both types of silk differed from one another in all characteristics except stiffness (Fig. 1).

The mechanical properties of silks are thought to be strongly affected by the internal organization of the molecules constituting these polymer fibers. A growing body of evidence suggests that each type of fiber is spun from a unique set of fibroins (e.g. Garb and Hayashi, 2005; Gatesy et al., 2001; Guerette et al., 1996; Hayashi et al., 2004; Hayashi and Lewis, 2000). The fibroin sequences may largely determine a specific molecular organization of each fiber (Gosline et al., 1999). If so, then the variation among the sequences of spider silk fibroins could account for much of the variation that we found in mechanical performance (Table 3). For instance, major ampullate and minor ampullate silk fibroins share many similarities in molecular elements, particularly both contain glycine- and alanine-rich motifs that form crystalline β-sheets (Table 3), whereas other silks either have much lower frequencies of these motifs or lack them entirely. The mechanical performance of major ampullate and minor

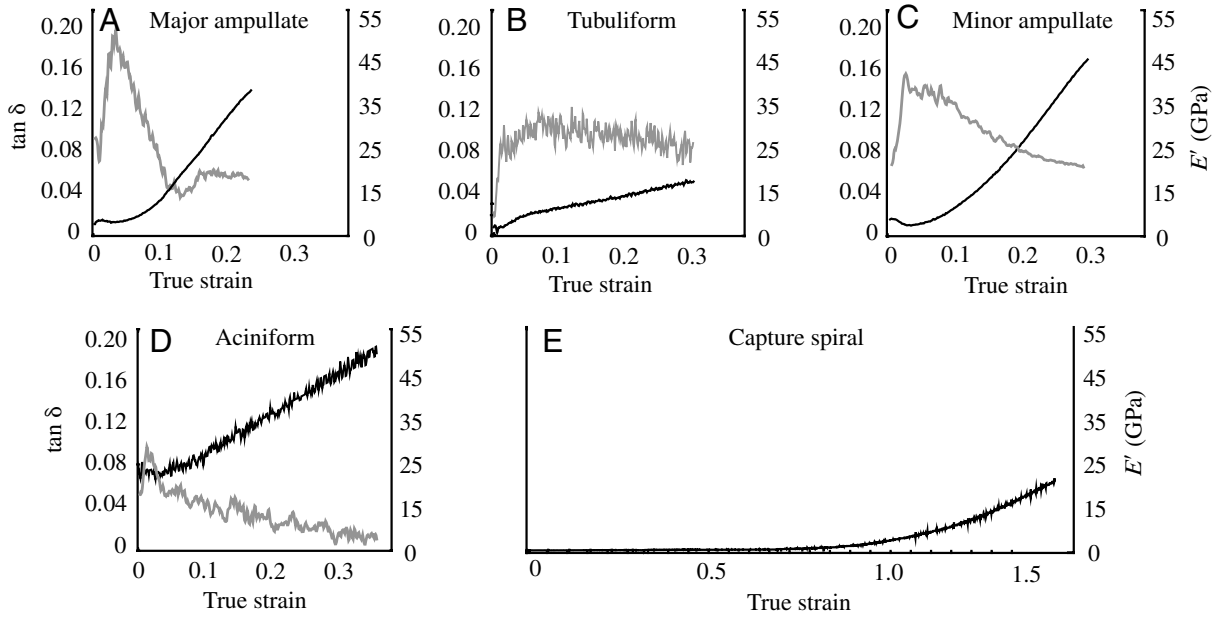

Fig. 5. Exemplar dynamic mechanical curves for each of the five fibrous silks spun by *Argiope argentata*. Gray denotes the loss tangent (tan δ) and black denotes the storage modulus (E'). Loss tangent could not be measure effectively for capture spiral due to the extremely low magnitude of the loss modulus. Note the difference in the scale of the *x* axis for capture spiral (E) relative to other types of silk (A–D).

ampullate silk fibers are qualitatively more similar to one another than to other silks (Figs 2 and 5). The dynamic performance of these two silks is also similar to one another and is consistent with previously hypothesized molecular models of silk fibroins that contain large numbers of poly-Ala or Gly-Ala amino acid sequence motifs (Blackledge et al., 2005c). In particular, the rapid linear increase in the loss tangent during fiber yield is consistent with the breaking of hydrogen bonds within the amorphous regions of fibers, which facilitates viscous flow during yield (Termonia, 1994). The subsequent drop in loss tangent is probably caused by an increase in energy stored within fibers, as molecules within the amorphous regions become increasingly oriented during extension of the fibers. The greater strength and decreased extensibility of major ampullate silk relative to minor ampullate silk may be related to the higher prevalence of poly-Ala motifs in major ampullate fibers, because these motifs are hypothesized to form a particularly strong crystalline secondary/tertiary structure (Simmons et al., 1996).

The frequency of poly-Ala motifs in major ampullate silk has been associated with high tensile strength, therefore the long, uninterrupted runs of Gly-Pro-Gly-containing motifs in flagelliform fibroins may explain much of the extreme extensibility of the capture spiral. The arrays of linked Gly-Pro-Gly motifs in flagelliform silk are hypothesized to form successive β-turns that function as molecular springs (Becker et al., 2003; Hayashi and Lewis, 1998).

Similarly, the low storage moduli of capture spiral and tubuliform silk at failure are consistent with the finding, based on circular dichroism spectra, that these two silks have weaker intermolecular interactions than minor and major ampullate fibroins (Dicko et al., 2004). Unlike other types of silk, aciniform and tubuliform fibroins are composed of very long, complex repeats instead of short, simple repeats of alanine and/or glycine rich motifs (Garb and Hayashi, 2005; Hayashi et al., 2004; Tian and Lewis, 2005). Currently there is little information available on the molecular structure of aciniform and tubuliform silks. However, our mechanical data suggest that aciniform and tubuliform silk fibers perform quite well in comparison to silks characterized by simple repeats. It is particularly interesting that tubuliform silk exhibits little post-yield hardening as this suggests that the observed twisting in the crystalline fraction of tubuliform fibers (Barghout et al., 1999) reduces energy storage, resulting in little post-yield change in storage modulus. More important, our data demonstrate that high performance biomimetic silk fibers can be synthesized without being constrained to large proportions of poly-Ala, Gly-Ala, or Gly-Pro-Gly motifs.

The relationship between the material properties of different spider silks to ecological function has received little attention. The clearest links so far involve the two best-studied silks, major ampullate and capture spiral. Major ampullate silk provides a dry frame that supports the sticky capture spiral of orb webs (Gosline et al., 1999; Vollrath, 1999). The high tensile strength and toughness of major ampullate and capture spiral silks make them both well-suited to resist the kinetic energy of flying insect prey. However, major ampullate silk is stronger and stiffer, but far less extensible, than the capture spiral. The extremely high compliance and extensibility of capture spiral silk helps ‘cradle’ insects upon impact so that insects decelerate gradually and do not bounce out of webs. During this process, the kinetic energy of the insects is absorbed through low initial resilience of both

Table 3. *Hypothesized relationships between molecular structure, mechanical performance, and ecological use of silks spun by Argiope argentata*

Silk	Molecular elements	Mechanical performance	Ecological function
Major ampullate	Composition: GA and poly(A) motifs, short repeats of $GPGX_n$ motifs[1,2] 2° structure: β-sheet crystals oriented along fiber axis embedded in amorphous matrix[3,4]	High tensile strength, low extensibility, high loss tangent, exhibits super contraction when wetted, higher hysteresis	Draglines, primary dry structural elements of most capture webs
Tubuliform	Composition: A and S rich, long and complex repeats lacking in subrepeat motifs[5,6] 2° structure: β-sheets twist parallel to fiber orientation embedded in amorphous matrix[3,7,8,9]	High modulus, low strength, very little stiffening after fiber yield, consistently low storage modulus, loss tangent is relatively constant after fiber yield, thick diameter	Inner flocculent silk of egg sacs
Minor ampullate	Composition: GA motifs lack poly(A) motifs[1] 2° structure: β-sheet crystals oriented along fiber axis embedded in amorphous matrix[9]	High modulus and extensibility, moderate tensile strength and toughness	Temporary spiral of orb, sometimes added to draglines
Aciniform	Composition: G, A and S rich, long, complex repeats lacking in subrepeat motifs[10] 2° structure: uncharacterized	High modulus, extensibility and toughness, high storage modulus, multi-strand sheet of fine fibers	Prey wrapping, stabilimentum web decorations, outer layer of egg sacs
Capture spiral	Composition: core fiber (flagelliform silk gland) coated with glycoprotenin glue, core fiber has long repeats of $GPGX_n$ motifs[11] 2° structure: lacks β-sheet, subrepeats fold into molecular 'nanosprings', plasticized fiber[12,13,14,15]	Extremely extensible and resilient, highly compliant, glue-coated wet fiber	Sticky spiral of ecribellate orb webs

Amino acids are indicated by one-letter abbreviations: A, alanine; G, glycine; P, proline; S, serine; X, glycine or other amino acid. [1](Gatesy et al., 2001), [2](Xu and Lewis, 1990), [3](Parkhe et al., 1997), [4](Thiel et al., 1997), [5](Garb and Hayashi, 2005), [6](Tian and Lewis, 2005), [7](Barghout et al., 2001), [8](Barghout et al., 1999), [9](Dicko et al., 2004), [10](Hayashi et al., 2004), [11](Hayashi and Lewis, 2000), [12](Gosline et al., 1984), [13](Hayashi and Lewis, 1998), [14](Hayashi and Lewis, 2001), [15](Vollrath and Edmonds, 1989).

capture spiral and major ampullate silk (Denny, 1976), coupled with aerodynamic dampening as the capture spiral stretches (Lin et al., 1995). The important role of the mechanical properties of these two silks for prey capture is also supported by the fact that both silks exhibit substantial evolutionary change in mechanical performance associated with differences among species of spiders in the architectures of orb webs (Craig, 1987; Opell and Bond, 2000; Opell and Bond, 2001). This suggests that the mechanical performance of these two silks may be 'fine-tuned' by the demands placed upon them by webs spun in different habitats or that capture different types of insect prey. However, major ampullate silk is used for a variety of other functions (Table 3), besides spinning orb webs, and phylogenetic evidence suggests that many of its high performance characteristics evolved prior to the origin of aerial orb webs (Swanson et al., 2006).

By contrast to prey-catching orb webs, the egg sacs of spiders function primarily as physical barriers to predators and the elements (Hieber, 1992a; Hieber, 1992b). Thus, the fibers need to be relatively stiff and strong to prevent eggs from being crushed (i.e. resist pressure), but do not necessarily need to be tough (i.e. absorb kinetic energy). These functional differences are reflected in our data where tubuliform silk has a relatively high initial modulus but stiffens little after the yield point (Fig. 2). To date, most spider silks characterized exhibit a strong capacity to store energy as they are strained post-yield so that the largely viscous post-yield behavior of tubuliform fibers is unusual (Fig. 5). One possible explanation is that tubuliform silk primarily functions to provide physical protection to eggs from parasites and predators. Any selection for physical performance under these circumstances would probably come from resisting pressure applied to egg sacs, which could result in the displacement of fibers within the flocculent silk next to the eggs. The largely viscous post-yield behavior of tubuliform fibers may prevent these fibers from recovering elastically after some traumatic deformation of the egg sac, which would prevent movement of the fibers themselves during elastic recovery acting as a second source of damage to eggs. Tubuliform fibers are also more irregular in cross-section than other silks, with small knobs and grooves on their surface (Fig. 6). Similar sculpturing has been found in the tubuliform silk of the related orb-weaver *Zygiella x-notata* (Gheysens et al., 2005), suggesting that it is a

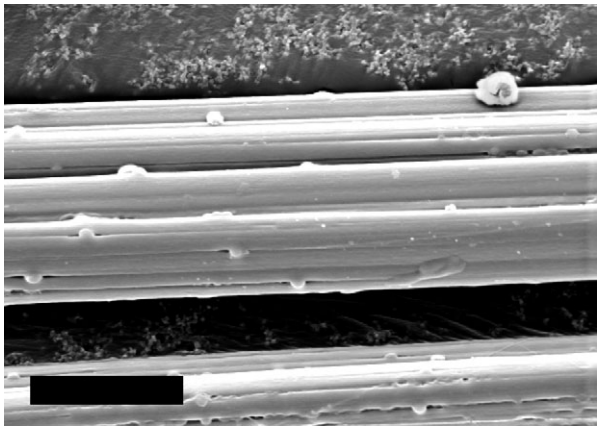

Fig. 6. Scanning electron microscope image of a fiber of tubuliform silk exhibiting characteristic grooves and nodules on its exterior. Bar, 5 μm.

common feature of this type of silk. It may even indicate a fibrillar substructure within the fibers. These irregular features probably increase the second moment of area of fibers thereby functioning to increase flexural stiffness of the fibers, much as steel I-beams resist bending better than steel rods.

Aciniform silk is remarkable, even among other spider silks, which already rank among the toughest fibers known, for its extreme toughness (Fig. 1). This is due in large part to the greater extensibility of aciniform fibers relative to other dry silks. This high toughness had been previously identified for the related species *Argiope trifasciata* (Forskal 1775) (Hayashi et al., 2004), and may play an important role in the function of this silk to swath struggling insect prey.

In summary, our study quantifies the mechanical and material properties of the fibrous silks spun by *Argiope argentata*. As a whole, the silks possess extraordinary properties, but are also strikingly diverse. These silks provide orb-weaving spiders with diverse toolkits of fibers that seem fine-tuned for particular ecological functions. This variety is reflected in not just the distinctive mechanical properties of each silk, but also in the underlying molecular structures and amino acid sequences of the fibroins. Precise characterization of all the fibers spun by a single species provides insight into the unique ways that orb weaving spiders can interact with their environment. Furthermore, the rich specializations that have evolved among the different silks spun by *Argiope* can be exploited to customize the mechanical properties of recombinant silks.

List of symbols

A	cross-sectional area of fibers
E'	storage modulus
F	force
L	instantaneous fiber length
L_o	fiber gage length
ϵ_t	true strain
σ_t	true stress

We thank Joy Sarkar for assistance. Awards DAAD19-02-1-0107 and DAAD19-02-1-0358 from the US Army Research Office supported this project. We are also grateful to two anonymous reviewers who supplied helpful suggestions that improved this manuscript.

References

Arcidiacono, S., Mello, C., Kaplan, D., Cheley, S. and Bayley, H. (1998). Purification and characterization of recombinant spider silk expressed in *Escherichia coli*. *Appl. Microbiol. Biotechnol.* **49**, 31-38.

Barghout, J. Y. J., Thiel, B. L. and Viney, C. (1999). Spider (*Araneus diadematus*) cocoon silk: a case of non-periodic lattice crystals with a twist? *Int. J. Biol. Macromol.* **24**, 211-217.

Barghout, J. Y. J., Czernuszka, J. T. and Viney, C. (2001). Multiaxial anisotropy of spider (*Araneus diadematus*) cocoon silk fibres. *Polymer* **42**, 5797-5800.

Becker, N., Oroudjev, E., Mutz, S., Cleveland, J. P., Hansma, P. K., Hayashi, C. Y., Makarov, D. E. and Hansma, H. G. (2003). Molecular nanosprings in spider capture-silk threads. *Nat. Mat.* **2**, 278-283.

Blackledge, T. A., Coddington, J. A. and Gillespie, R. G. (2003). Are three-dimensional spider webs defensive adaptations? *Ecol. Lett.* **6**, 13-18.

Blackledge, T. A. and Gillespie, R. G. (2004). Convergent evolution of behavior in an adaptive radiation of Hawaiian web-building spiders. *Proc. Natl. Acad. Sci. USA* **101**, 16228-16233.

Blackledge, T. A., Cardullo, R. A. and Hayashi, C. Y. (2005a). Polarized light microscopy, variability in spider silk diameters, and the mechanical characterization of spider silk. *Invertebr. Biol.* **124**, 165-173.

Blackledge, T. A., Summers, A. P. and Hayashi, C. Y. (2005b). Gumfooted lines in black widow cobwebs and the mechanical properties of spider capture silk. *Zoology* **108**, 41-46.

Blackledge, T. A., Swindeman, J. E. and Hayashi, C. Y. (2005c). Quasistatic and continuous dynamic characterization of the mechanical properties of silk from the cobweb of the black widow spider *Latrodectus hesperus*. *J. Exp. Biol.* **208**, 1937-1949.

Craig, C. L. (1987). The ecological and evolutionary interdependence between web architecture and web silk spun by orb web weaving spiders. *Biol. J. Linn. Soc. Lond.* **30**, 135-162.

Craig, C. L. (2003). *Spider Webs And Silk: Tracing Evolution from Molecules to Genes to Phenotypes*. New York: Oxford University Press.

Cunniff, P. M., Fossey, S. A., Auerbach, M. A. and Song, J. W. (1994). Mechanical properties of major ampulate gland silk fibers extracted from *Nephila clavipes* spiders. In *Silk Polymers*. Vol. 544 (ed. D. Kaplan, W. W. Adams, B. Farmer and C. Viney), pp. 234-251. Washington, DC: American Chemical Society.

Denny, M. (1976). Physical properties of spider silks and their role in design of orb-webs. *J. Exp. Biol.* **65**, 483-506.

Dicko, C., Knight, D., Kenney, J. M. and Vollrath, F. (2004). Secondary structures and conformational changes in flagelliform, cylindrical, major, and minor ampullate silk proteins. Temperature and concentration effects. *Biomacromolecules* **5**, 2105-2115.

Dunaway, D. L., Thiel, B. L., Srinivasan, S. G. and Viney, C. (1995). Characterizing the cross-sectional geometry of thin, noncylindrical, twisted fibers (spider silk). *J. Mat. Sci.* **30**, 4161-4170.

Foelix, R. F. (1996). *Biology of Spiders.* New York: Oxford University Press.

Foo, C. W. P. and Kaplan, D. L. (2002). Genetic engineering of fibrous proteins: spider dragline silk and collagen. *Adv. Drug Deliv. Rev.* **54**, 1131-1143.

Garb, J. E. and Hayashi, C. Y. (2005). Modular evolution of egg case silk genes across orb-weaving spider superfamilies. *Proc. Natl. Acad. Sci. USA* **102**, 11379-11384.

Garrido, M. A., Elices, M., Viney, C. and Pérez-Rigueiro, J. (2002). Active control of spider silk strength: comparison of drag line spun on vertical and horizontal surfaces. *Polymer* **43**, 1537-1540.

Gatesy, J., Hayashi, C., Motriuk, D., Woods, J. and Lewis, R. (2001). Extreme diversity, conservation, and convergence of spider silk fibroin sequences. *Science* **291**, 2603-2605.

Gheysens, T., Beladjal, L., Gellynck, K., Van Nimmen, E., Van Langenhove, L. and Mertens, J. (2005). Egg sac structure of *Zygiella x-notata* (Arachnida, Araneidae). *J. Arachnol.* **33**, 549-557.

Gosline, J. M., Denny, M. W. and Demont, M. E. (1984). Spider silk as rubber. *Nature* **309**, 551-552.

Gosline, J. M., Pollak, C. C., Guerette, P. A., Cheng, A., Demont, M. E. and Denny, M. W. (1994). Elastomeric network models for the frame and viscid silks from the orb web of the spider *Araneus diadematus*. In *Silk Polymers*. Vol. 544 (ed. D. Kaplan, W. W. Adams, B. Farmer and C. Viney), pp. 328-341. Washington, DC: American Chemical Society.

Gosline, J. M., Guerette, P. A., Ortlepp, C. S. and Savage, K. N. (1999). The mechanical design of spider silks: from fibroin sequence to mechanical function. *J. Exp. Biol.* **202**, 3295-3303.

Guerette, P. A., Ginzinger, D. G., Weber, B. H. F. and Gosline, J. M. (1996). Silk properties determined by gland-specific expression of a spider fibroin gene family. *Science* **272**, 112-115.

Hayashi, C. Y. and Lewis, R. V. (1998). Evidence from flagelliform silk cDNA for the structural basis of elasticity and modular nature of spider silks. *J. Mol. Biol.* **275**, 773-784.

Hayashi, C. Y. and Lewis, R. V. (2000). Molecular architecture and evolution of a modular spider silk protein gene. *Science* **287**, 1477-1479.

Hayashi, C. Y. and Lewis, R. V. (2001). Spider flagelliform silk: lessons in protein design, gene structure, and molecular evolution. *BioEssays* **23**, 750-756.

Hayashi, C. Y., Shipley, N. H. and Lewis, R. V. (1999). Hypotheses that correlate the sequence, structure, and mechanical properties of spider silk proteins. *Int. J. Biol. Macromol.* **24**, 271-275.

Hayashi, C. Y., Blackledge, T. A. and Lewis, R. V. (2004). Molecular and mechanical characterization of aciniform silk: uniformity of iterated sequence modules in a novel member of the spider silk fibroin gene family. *Mol. Biol. Evol.* **21**, 1950-1959.

Hieber, C. S. (1992a). The role of spider cocoons in controlling desiccation. *Oecologia* **89**, 442-448.

Hieber, C. S. (1992b). Spider cocoons and their suspension systems as barriers to generalist and specialist predators. *Oecologia* **91**, 530-535.

Huemmerich, D., Scheibel, T., Vollrath, F., Cohen, S., Gat, U. and Ittah, S. (2004). Novel assembly properties of recombinant spider dragline silk proteins. *Curr. Biol.* **14**, 2070-2074.

Kaplan, D., Adams, W. W., Farmer, B. and Viney, C. (1994). Silk-biology, structure, properties, and genetics. In *Silk Polymers.* Vol. 544 (ed. D. Kaplan, W. W. Adams, B. Farmer and C. Viney), pp. 2-16. Washington, DC: American Chemical Society.

Kitagawa, M. and Kitayama, T. (1997). Mechanical properties of dragline and capture thread for the spider *Nephila clavata*. *J. Mat. Sci.* **32**, 2005-2012.

Köhler, T. and Vollrath, F. (1995). Thread biomechanics in the two orb-weaving spiders *Araneus diadematus* (Araneae, Araneidae) and *Uloborus walckenaerius* (Araneae, Uloboridae). *J. Exp. Zool.* **271**, 1-17.

Lazaris, A., Arcidiacono, S., Huang, Y., Zhou, J. F., Duguay, F., Chretien, N., Welsh, E. A., Soares, J. W. and Karatzas, C. N. (2002). Spider silk fibers spun from soluble recombinant silk produced in mammalian cells. *Science* **295**, 472-476.

Lewis, R. V., Hinman, M., Kothakota, S. and Fournier, M. J. (1996). Expression and purification of a spider silk protein: a new strategy for producing repetitive proteins. *Protein Expr. Purif.* **7**, 400-406.

Lin, L. H., Edmonds, D. T. and Vollrath, F. (1995). Structural engineering of an orb-spider's web. *Nature* **373**, 146-148.

Madsen, B. and Vollrath, F. (2000). Mechanics and morphology of silk drawn from anesthetized spiders. *Naturwissenschaften* **87**, 148-153.

Opell, B. D. and Bond, J. E. (2000). Capture thread extensibility of orb-weaving spiders: testing punctuated and associative explanations of character evolution. *Biol. J. Linn. Soc. Lond.* **70**, 107-120.

Opell, B. D. and Bond, J. E. (2001). Changes in the mechanical properties of capture threads and the evolution of modern orb-weaving spiders. *Evol. Ecol. Res.* **3**, 567-581.

Ortlepp, C. S. and Gosline, J. M. (2004). Consequences of forced silking. *Biomacromolecules* **5**, 727-731.

Parkhe, A. D., Seeley, S. K., Gardner, K., Thompson, L. and Lewis, R. V. (1997). Structural studies of spider silk proteins in the fiber. *J. Mol. Recognit.* **10**, 1-6.

Pérez-Rigueiro, J., Elices, M., Llorca, J. and Viney, C. (2001). Tensile properties of *Argiope trifasciata* drag line silk obtained from the spider's web. *J. Appl. Polym. Sci.* **82**, 2245-2251.

Simmons, A. H., Michal, C. A. and Jelinski, L. W. (1996). Molecular orientation and two-component nature of the crystalline fraction of spider dragline silk. *Science* **271**, 84-87.

Sirichaisit, J., Young, R. J. and Vollrath, F. (2000). Molecular deformation in spider dragline silk subjected to stress. *Polymer* **41**, 1223-1227.

Stauffer, S. L., Coguill, S. L. and Lewis, R. V. (1994). Comparison of the physical properties of three silks from *Nephila clavipes* and *Araneus gemmoides*. *J. Arachnol.* **22**, 5-11.

Swanson, B. O., Blackledge, T. A., Beltrán, J. and Hayashi, C. Y. (2006). Variation in the material properties of spider dragline silk across species. *Appl. Phys. A Mat. Sci. Proc.* **82**, 213-218.

Termonia, Y. (1994). Molecular modeling of spider silk elasticity. *Macromolecules* **27**, 7378-7381.

Thiel, B. L., Guess, K. B. and Viney, C. (1997). Non-periodic lattice crystals in the hierarchical microstructure of spider (major ampullate) silk. *Biopolymers* **41**, 703-719.

Tian, M. Z. and Lewis, R. V. (2005). Molecular characterization and evolutionary study of spider tubuliform (eggcase) silk protein. *Biochemistry* **44**, 8006-8012.

Van Nimmen, E., Gellynck, K., Gheysens, T., Van Langenhove, L. and Mertens, J. (2005). Modeling of the stress-strain behavior of egg sac silk of the spider *Araneus diadematus*. *J. Arachnol.* **33**, 629-639.

Vollrath, F. (1999). Biology of spider silk. *Int. J. Biol. Macromol.* **24**, 81-88.

Vollrath, F. and Edmonds, D. T. (1989). Modulation of the mechanical properties of spider silk by coating with water. *Nature* **340**, 305-307.

Vollrath, F. and Knight, D. P. (1999). Structure and function of the silk production pathway in the spider *Nephila edulis*. *Int. J. Biol. Macromol.* **24**, 243-249.

Vollrath, F., Knight, D. P. and Hu, X. W. (1998). Silk production in a spider involves acid bath treatment. *Proc. Natl. Acad. Sci. USA* **265**, 817-820.

Vollrath, F., Madsen, B. and Shao, Z. Z. (2001). The effect of spinning conditions on the mechanics of a spider's dragline silk. *Proc. Natl. Acad. Sci. USA* **268**, 2339-2346.

Winkler, S., Szela, S., Avtges, P., Valluzzi, R., Kirschner, D. A. and Kaplan, D. (1999). Designing recombinant spider silk proteins to control assembly. *Int. J. Biol. Macromol.* **24**, 265-270.

Work, R. W. (1976). Force–elongation behavior of web fibers and silks forcibly obtained from orb-web-spinning spiders. *Text. Res. J.* **46**, 485-492.

Work, R. W. (1977). Dimensions, birefringences, and force-elongation behavior of major and minor ampullate silk fibers from orb-web-spinning spiders – the effects of wetting on these properties. *Text. Res. J.* **47**, 650-662.

Xu, M. and Lewis, R. V. (1990). Structure of a protein superfiber – spider dragline silk. *Proc. Natl. Acad. Sci. USA* **87**, 7120-7124.